Combust. Sci. and Tech., 1991, Vol. 75, pp. 179–194
Photocopying permitted by license only

Non-Intrusive Measurement of Gaseous Species in Reacting and Non-Reacting Sprays

M. ADACHI*, V.G. McDONELL, and G.S. SAMUELSEN† *UCI Combustion Laboratory, University of California, Irvine, CA 92717 USA*

(Received January 5, 1990; in final form September 10, 1990)

Abstract—A non-intrusive technique for measuring the concentration of gaseous species in reacting and non-reacting sprays is presented. Infrared absorption is the basis for the measurement. In a two-phase situation, the light scattered by particles can be deduced by measuring extinction of wavelengths at which no absorption occurs. As a result, combined infrared extinction and scattering (IRES) is employed for two-phase flows. The technique, although based on line-of-sight absorption, has the potential to be spatially-resolved for either symmetric or asymmetric fields depending upon the deconvolution technique applied. The technique is demonstrated using a single phase methanol vapor/air free jet and non-reacting and reacting methanol sprays. To complement these results, measurements of droplet size and velocity as well as gas velocity can be achieved using other non-intrusive approaches such as phase Doppler interferometry. These complementary measurements may be combined with the concentration measurements to quantify vaporization. The results illustrate the applicability of this relatively inexpensive and simple technique which adds valuable information to the study of sprays.

INTRODUCTION

Detailed studies of the interaction between the gas phase and drops within sprays are required to understand the physical processes occurring, such as droplet transport, evaporation, fuel/air mixing, and combustion. Recently, experimental techniques for the characterization of drop behavior in sprays, such as phase Doppler interferometry, have evolved to the point where significant detailed information is obtained such as drop size and drop velocity (*e.g.*, Bachalo and Houser, 1984; McDonell and Samuelsen, 1988). Interaction of the drops with the gas phase in terms of velocity and momentum exchange is also being addressed in some detail via these same laser diagnostic techniques (*e.g.*, McDonell and Samuelsen, 1988, 1989).

The measurement of the gaseous species concentration within a spray would be invaluable as well. Although phase Doppler interferometry can, in principle, evaluate evaporation of the liquid via mass conservation considerations, limitations in the absolute accuracy of the volume flux measurement and variation in the symmetry of sprays restrict its use in this role. Further, phase Doppler is not capable of measuring other gaseous species (*e.g.*, CO_2 and CO in reacting sprays).

Mechanical probes have been used to measure gaseous species in both reacting and non-reacting sprays, but can perturb the flow and may not satisfactorily separate the two-phases (*e.g.*, Owen, *et al.*, 1978). Progress has been made in the non-intrusive measurement of species concentration in non-reacting sprays including light extinction by vapor absorption and drop scattering combined with light extinction by drop scattering alone to discriminate between drops and vapor in a spray (Chraplyvy, 1981). However, Chraplyvy provides little detail about the methodology or sources of error associated with the technique. Melton and Verdieck (1984) utilize exiplex fluorescence systems to discriminate phase. The exiplex system, which results from the

*Visiting Scientist, Horiba, Ltd., Kyoto Japan.
†Corresponding Author.

introduction of an organic dye into the liquid, causes the fluorescence wavelength of vapor and liquid to be distinct. The primary drawbacks to the approach are that (1) it is not suited for reacting environments and (2) the vaporization characteristics of the dye/liquid must be very well known. More recently, Allen and Hanson (1986) used planar laser-induced fluorescence (PLIF) and planar multi-photon dissociation (PMPD). This latter approach is capable of providing instantaneous measurements of a variety of gaseous species within reacting sprays, but is relatively expensive and limited in spatial resolution and absolute accuracy.

The present technique utilizes the concept of Chraplyvy (1981) but employs a broadband light source. The broadband source permits additional species to be interrogated besides the hydrocarbon vapor and, as such, makes the instrument well suited for characterization of species present in reacting flows as well as non-reacting flows. The broadband light source also provides an alternative means of correcting for the wavelength dependent scattering of the background measurement.

The objective of the present paper is to provide a description of a relatively inexpensive optical probe which can be used for characterization of gaseous species present in an arbitrary particle laden flow (*e.g.*, spray) under reacting or non-reacting conditions. As an example, the diagnostic is applied to (1) a single phase methanol vapor/air jet, (2) a non-reacting methanol spray, and (3) the same methanol spray under reacting conditions.

CONCEPT OF THE MEASUREMENT

Theory

The concentration of gaseous species within a gas/particle two-phase flow is determined using infrared extinction/scattering (IRES). Light propagating in such a flow is subject to extinction via scattering and absorption. The scattering is due to particles and consists of diffraction, refraction, and reflection. The absorption mechanism contains information from which the concentration of a select material may be determined.

The treatment of the scattering depends upon the size of the particles. If the size parameter, $\pi D/\lambda$, is greater than 10, where D is the diameter of the particle and λ is the wavelength, it is generally accepted that (1) the above modes of scattering can be separated and (2) diffraction contains the majority of the scattered energy (van de Hulst, 1985). Thus, in regions of many sprays, reflection and refraction may be neglected, expecially in the forward direction. This, however, is not true in general and, if the liquid absorbs light of the same wavelength as the gaseous species within the spray, the effect must be carefully examined.

The primary challenge is distinguishing between the scattering and possible absorption by the drops and the gas phase absorption. One way is to measure the scattering at a wavelength for which no gas absorption occurs and then compensate for the wavelength dependency of the scattering. In principle, the wavelength dependency can be calculated using Mie theory for the drop size distribution present in the spray, which can either be measured, or derived empirically. This is not desirable because the ability to measure the size distribution along the light path with high accuracy can be quite challenging in itself. As a result, the dependency is evaluated in another fashion, namely, using two wavelengths about the probe wavelength to "window" the probe wavelength. This will be explained in more detail in the application section.

Once the extinction due solely to the gas phase is known, the results are translated into the absorbance. The extinction of a ray of light transmitted through a medium

is described by Lambert-Beer's law:

$$I = I_0 e^{-\alpha}, \tag{1}$$

where I is the transmitted light intensity, I_0 the incident light intensity, and α is the absorbance which is a product of gas concentration, optical path length, and the absorption coefficient of the material of interest.

Solving Eq. (1) for α and letting $\alpha = \alpha(x_i)$, $I_0 = I_{\text{scatter}}(x_i)$, and $I = I_{\text{probe}}(x_i)$, leads to Eq. (2), which determines the gas absorbance:

$$\alpha(x_i) = \text{Log}\,(I_{\text{scatter}}(x_i)/I_{\text{probe}}(x_i)), \tag{2}$$

where x_i indicates the radial position at which the line-of-sight measurement is obtained. In a particle ladened flow, $I_{\text{scatter}}(x_i)$ must be implicitly determined as described above. In a single phase case, $I_{\text{scatter}}(x_i)$ is replaced with $I_{\text{probe}}(x_i)$ measured with no sample present. The absorbance value is converted to gas concentration via calibration. In cases where the species to be studied is common, span gases may be available which can be used for calibration purposes.

The technique is based upon a line-of-sight measurement, but deconvolution approaches, ranging from "onion-peeling" to two-dimensional Fourier transforms (*e.g.*, Chen and Goulard, 1976: Santoro, *et al.*, 1981), may be applied to obtain spatially resolved information in sprays of arbitrary symmetry.

In principle, any kind of gas that has absorption bands in the infrared can be measured (*e.g.*, hydrocarbon vapors, CO_2, H_2O, and NO). For example, most hydrocarbons absorb light 3.5 μm in wavelength, and CO_2 absorbs light 4.3 μm in wavelength. These wavelengths can be detected with relatively inexpensive photo cells. NO (5.4 μm) can be measured with a cryogenically cooled MCT (Mercury Cadmium Teluride) detector which is relatively expensive. Further, a monochromator or a spectrometer might be used to investigate multiple species with one measurement. FT–IR would be appropriate for extremely steady flows (*e.g.* Solomon, *et al.*, 1986) but would not be suitable for a typical spray. In each case, droplet extinction at the probe wavelength must be evaluated using either Mie theory combined with a measured droplet size distribution or by using "windowing wavelengths." In reacting cases, wavelength windowing may not be feasible due to existence of various combustion products which may interfere with the measurement. In cases where interference is possible, additional wavelengths can provide another background. Alternatively, Mie theory combined with drop size distributions can still be used, which then renders the technique applicable only to spherical particles. Interference by infrared emission can also occur when measuring combustion products in the reacting conditions. In this case, the interference can be cancelled with a measured emission background without using the light source.

APPLICATION TO METHANOL

Protocol

For both liquid and gaseous methanol, a strong absorption band exists from 2750 to 3100 cm^{-1} (3.2 to 3.6 μm) which is typical of most hydrocarbons (Figure 1a). The absorption spectra of liquid and gaseous methanol reveal several differences including a 3700 cm^{-1} (2.7 μm) absorption peak due to OH-stretching vibration for gas phase which becomes a 3350 cm^{-1} (2.99 μm) broad band absorption for the liquid phase.

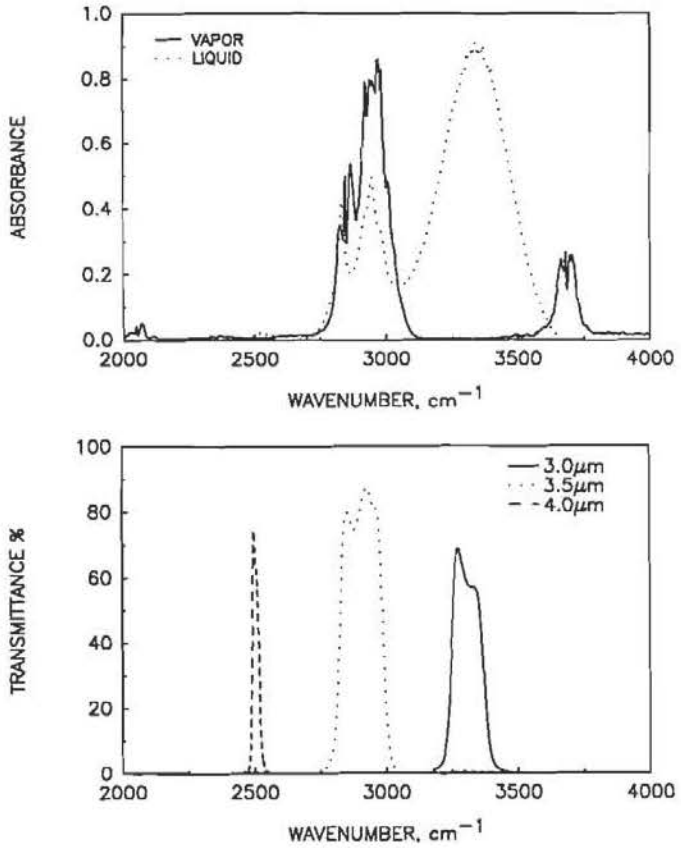

FIGURE 1 IR Spectra for Materials Used. a) Absorption for Gaseous and Liquid Methanol. b) Transmittance of Bandpass Filters.

This change occurs because of hydrogen bonding which does not exist in the gas phase. In principle, it is possible to take advantage of this difference in the gas and liquid absorption spectra to discriminate between the liquid and gaseous methanol, however, scattering makes liquid absorption measurements impractical.

The mean value of the 3.0 μm and 4.0 μm transmittances is used to determine the scattering at 3.5 μm. Figure 1b shows the transmittance profiles of the three filter used in the present study (4.0 μm: OCLI Filter No. 3997–4A; 3.5 μm: Horiba HC filter; 3.0 μm: Micro Coatings IR1–30–9LEY). This selection is made assuming that the liquid absorption at 3.0 μm and 3.5 μm is negligible (*i.e.*, diffraction is the dominant mode of scatter), as discussed in the error analysis section.

The single beam IR radiometry system used is shown in Figure 2. A relatively inexpensive heat coil light source, a CaF_2 collimating lens, an optical chopper operating at 1 kHz, and a spatial filter are used in the transmitter. The 4 mm diameter IR beam goes through the spray field and the desired wavelength is selected using various optical band pass filters. Each of the 3.0 μm, 3.5 μm and 4.0 μm band pass filters is used to establish light of a desired wavelength. The transmitted light is focused by a receiving lens onto a 1 mm^2 PbSe detector surface. The detector is mounted inside a thermally stabilized housing to minimize response drift. The detector output signal is fed to an ultra low noise preamplifier (EG&G Model 5003), which is in turn fed into

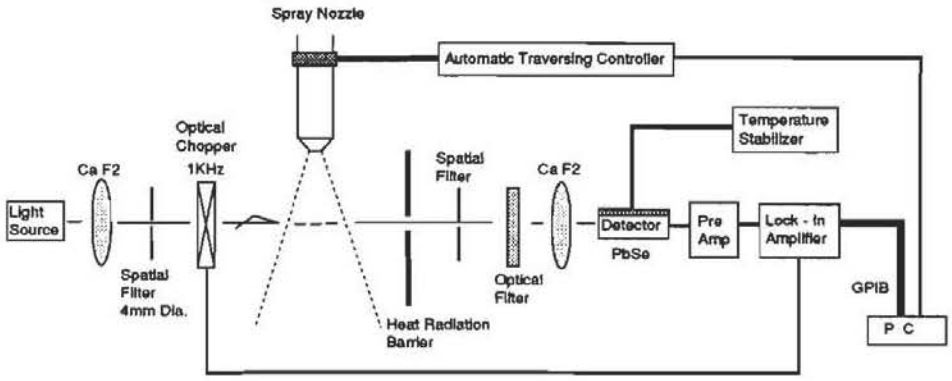

FIGURE 2 Single Beam IR Radiometry System for Spray.

a lock-in amplifier (EG&G Model 5205) operated at a time constant of 30 msec and a roll off rate 12 dB/octave.

A computer interface enables the user to select (1) the averaging time used to make up one itensity measurement at a given location and (2) the positions at which data are to be acquired. The PC also controls traversing of the sample being tested. The subsequent position and absorption measurements are stored in files which are processed for wavelength compensation and background and then transformed into gas absorption via software developed for this purpose.

Single line-of-sight transmittances for the three filters are collected in 5 mm steps across a given axial location within the flow field shown in Figure 3a. A sampling period of 18 sec is used with a sampling rate of ~ 20 Hz to time-average transient behavior of the spray. The gas absorbance for each radial scan as shown in Figure 3b is calculated from Eq. (2) as described above.

An "onion-peeling" deconvolution scheme is used in the present axisymmetric case studies. The circular field is divided into n equally spaced rings each of which is assumed to possess homogeneous properties. Each line-of-sight absorption is written as

$$\alpha(x_i) = \varepsilon \Sigma_j L_{ij} C_j, \tag{3}$$

where ε is the absorption coefficient of the gas, L_{ij} is the optical path length of the jth ring, and C_j is the concentration of the jth ring. Using matrix notation, Eq. (3) can be expressed as

$$[\alpha] = \varepsilon [L][C], \tag{4a}$$

which can be inverted to yield the concentration at each position x_j using Eq. (4a).

$$[C] = 1/\varepsilon [L]^{-1} [\alpha]. \tag{4b}$$

Because $[L]$ appears as an $n \times n$ matrix with triangular elements, Eq. (4b) can be solved iteratively. The algorithm used in the present case first interpolates the gas absorption profile, $\alpha(x_i)$ using a cubic spline routine. These interpolated data give virtual spatial resolution which makes the width of each ring smaller and greatly reduces deconvolution error.

Span gases for methanol are available only in low concentrations. Without a

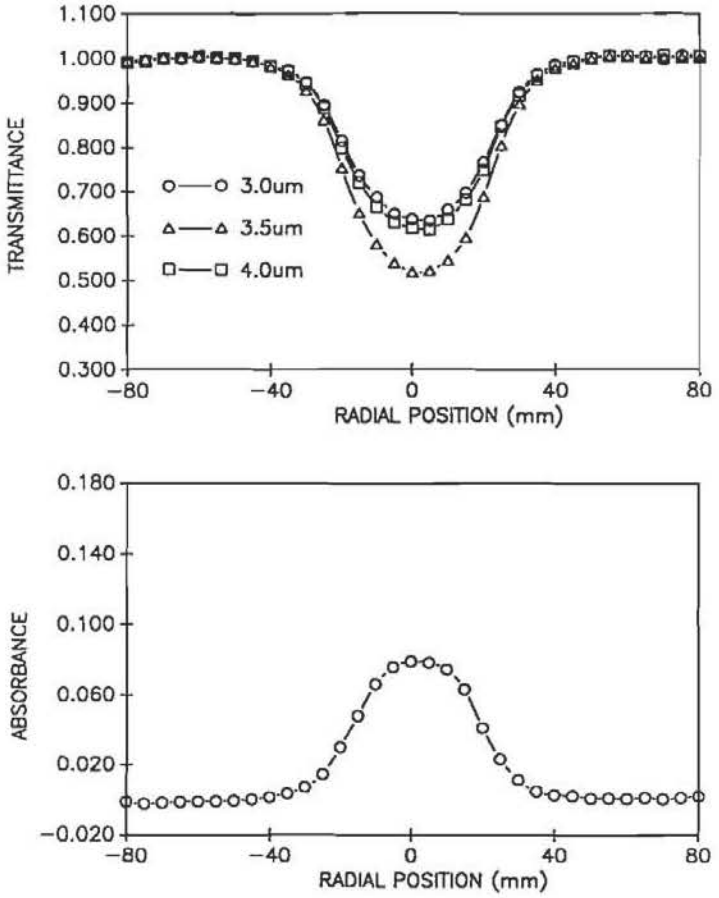

FIGURE 3 Typical Line-of-Sight Transmittance Profiles. a) Individual Transmittance for Three Filters. b) Difference in Transmittance for 3.5 micron filter and Mean Transmittance for 3.0 and 4.0 micron Filters.

suitable long pass gas cell, a calibration device can be applied. The high concentration calibration setup developed for the present case is shown in Figure 4. Nitrogen gas is bubbled through liquid methanol in a beaker at a known temperature and is then fed to a gas cell of known length. The vapor in the cell is measured by the non-intrusive IRES technique. Then, the absorbance for the particular concentration of the gas determined by vapor pressure is calculated and used to determine the absorption coefficient.

Error Analysis

Errors in the present approach may arise due to several factors, including (1) liquid phase absorption at 3.0 μm and 3.5 μm, (2) use of the mean transmittance of 3.0 and 4.0 μm light to represent the scattering of 3.5 μm light, (3) variation of optical properties of both the gas phase (beam steering effects) and drops with temperature, (4) interference from combustion products in the reacting case, (5) systematic variation, and (6) inherent inaccuracies in the deconvolution scheme (*e.g.*, assumption of symmetry).

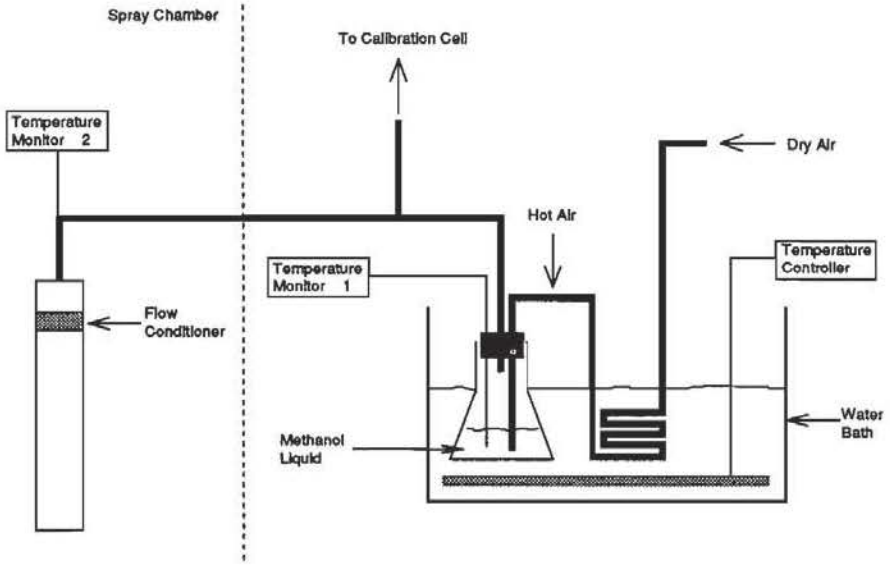

FIGURE 4 High Concentration Methanol Gas Calibration Setup.

It is not appropriate to evaluate the effect of liquid phase absorption at 3.0 and 3.5 μm using the absorption spectra shown in Figure 1a because scattering is not taken into account. To account for both the scattering and absorption, the size distribution must be known. Five size distributions were created which range from extremely fine drops, to ones measured by diffraction at different points in the spray considered later. The optical properties of methanol in the IR at 0° C are taken from Sethna and Williams (1979). To account for the variation in refractive index, absorptivity, and transmittance over the wavelengths of light passed by each filter, the transmission band is discretized into 0.2 μm intervals, and the appropriate transmission, refractive index, and absorptivity were selected. These values were used in a Mie scattering calculation (Wood, *et al.*, 1987) to determine $I(d)/I_0$ for drop sizes ranging from 1 to 100 μm. The values of $I(d)/I_0$ were then multiplied by the probability distribution for each size distribution and summed to give the total value of light received by the detector. The calculated results are summarized in Table I.

The results from Table I are consistent with the understanding of the light scattering, namely that only fine particles (Case 2) cause significant error in the assumption that liquid phase absorption is negligible. Case 1 is representative of the centerline diffraction measurement obtained in the spray in the present study.

Although the values in Table I are useful to establish the impact of liquid absorption, the values presented are not used directly to determine the concentration. Rather, the average of the 3.0 and 4.0 μm transmittance is used to determine the scattering due to drops. The error in concentration is then due to errors associated with this average value obtained using the "windowing" approach.

The windowing approach is evaluated in the same manner as above, where the optical properties of Sethna and Williams (1979) are used for each of the three wavelengths. Table II summarizes the error due to using the mean value of the transmittance of 3.0 and 4.0 to represent 3.5 μm light which is scattered and absorbed by the liquid, but not absorbed by the gas.

For the larger size distributions, the error presented in Table II could be reduced by using a relationship in the form $A(I_{3.0}) + B(I_{4.0})/(A + B)$ to represent $I_{3.5}$. The

TABLE I
Summary of Effect of Liquid Phase Absorption.

Case[a]	X^b	q^c	λ^d	n^e	k^f	I/I_0^g	% Transmittance Variation[h]
1	44.2	1.95	3.0	1.33	0.105	2.33	
			3.0	1.33	0.0	2.39	+2.5
			3.5	1.35	0.054	1.84	
			3.5	1.35	0.0	1.89	+2.7
2	20	3.0	3.0	1.33	0.105	1.22	
			3.0	1.33	0.0	1.30	+6.6
			3.5	1.35	0.054	0.98	
			3.5	1.35	0.0	1.05	+7.1
3	55	2.0	3.0	1.33	0.105	2.66	
			3.0	1.33	0.0	2.71	+1.9
			3.5	1.35	0.054	2.09	
			3.5	1.35	0.0	2.13	+1.9
4	90	1.5	3.0	1.33	0.105	2.09	
			3.0	1.33	0.0	2.13	+1.9
			3.5	1.35	0.054	1.64	
			3.5	1.35	0.0	1.67	+1.8
5	90	3.0	3.0	1.33	0.105	2.92	
			3.0	1.33	0.0	2.95	+1.0
			3.5	1.35	0.054	2.28	
			3.5	1.35	0.0	2.30	+0.8

[a]Model size distribution
[b]Rosin-Rammler size parameter
[c]Rosin-Rambler spread factor
[d]Wavelength, μm
[e]Real part of refractive index
[f]Absorption part of refractive index
[g]Ratio of light detected to original light intensity multiplied by 10^{12}
[h]Amount of extinction due to liquid absorption

3.3% error for Case 2 illustrates that the liquid phase absorption does become important as the drops become smaller. However, the error is still relatively small. Also, the windowing approach appears to reduce the maximum errors associated with the liquid absorption compared to using the Mie calculation.

The effect of temperature change is difficult to establish because no temperature dependent values of the optical properties of methanol in the IR are available in the literature. Empirical relationships, such as the Eyckman relation $[(n_{0.589}^2-1)/\rho\,(n_{0.589}+0.4) = \text{constant}$, where ρ is the density of the material and $n_{0.589}$ is the real

TABLE II
Summary of Results using Mean of 3.0 and 4.0.

Case[a]	$I_{3.5}/I_0^b$	$(I_{3.0}+I_{4.0})/2\ I_0$	% difference
1	1.84	1.88	2.2
2	0.98	1.013	3.3
3	2.09	2.14	2.2
4	1.64	1.68	2.1
5	2.28	2.33	2.2

[a]same as Table I.
[b]values multiplied by 10^{12}

part of the refractive index at the sodium D line], show that the real part of the refractive index of methanol at 0.589 μm varies from 1.34 at 0° C to 1.31 at 64.7° C (boiling point). However, the Eyckman relation may not be valid in the IR, and the amount of variation in the extinction part of the refractive index is unknown. To establish a conservative error, Mie calculations were conducted for a range of refractive indices (the real part was reduced by 0.05, and extinction part doubled) for the three wavelengths. The results show a maximum error of 7.5% when using windowing and the distribution of Case 2.

The impact of beam steering was investigated by making a transmission profile far downstream in the reacting spray at 4.0 μm where no absorption should occur. The transmittance profile remains flat, indicating that beam steering does not impact the results. For the operating condition in the present case, emission of IR light at each of the three wavelengths from the reacting spray is negligible.

Interference from combustion species (H_2O has an absorption band within the 3.0 μm band pass) can only be estimated in the present case. In the worst case, the transmittance of the 3.0 μm light is reduced to the same level the 4.0 μm light, in which case errors of up to 24% can occur. However, in most regions of the present reacting spray, the error due to the water band is much less. Also, a band where only water absorbs can be measured and readily used to correct the 3.0 μm transmittance.

Repeatability was examined using the 4.0 μm filter which gives the smallest throughput among the three filters. In the present spray, the intensity measurement converges within 0.2% using 256 samples. Repeatability of the system is 0.5% within one hour and the noise rms value outside the spray is less than 0.3%.

A 2% error in concentration is associated with the calibration procedure (it would be less with the use of span gases and long path length gas cells). Errors due to asymmetries and the deconvolution procedure are estimated to be less than 5% (based on radially offsetting the measured profile 2 mm from the "real" centerline).

Overall, the total error associated with the present spray and measurement protocol is 7% and about 12% for the non-reacting spray and reacting spray, respectively. Higher errors exist in the reacting case due to water band interference, but (1) the vapor concentration in these regions is very small, and (2) the water band interference can be corrected.

Results from Single Phase Jet

Figure 4 shows a schematic of the single phase pipe flow used in a test study. The results obtained at the exit plane (5 mm downstream) of the 25.4 mm diameter pipe are presented in Figure 5. Care was taken to ensure that saturated methanol vapor at a known temperature was present in the air.

The absorption profile present in Figure 5a reveals the well behaved property expected for this case. Subsequent deconvoltuion of these data lead to the concentration profile presented in Figure 5b. The temperature of the saturated gas in the pipe was measured at 26° C $\pm$ 1.5° C. This corresponds to a vapor concentration of 16.8 $\pm$ 1.4%. Hence, the results for this simple case are quite satisfactory, considering errors in the calibration.

Results from Methanol Spray

Details regarding the methanol spray considered are given elsewhere (McDonell, Adachi, and Samuelsen, 1990). For reference, Figure 6 presents a schematic of the spray structure studied under reacting and non-reacting conditions. The thick line on

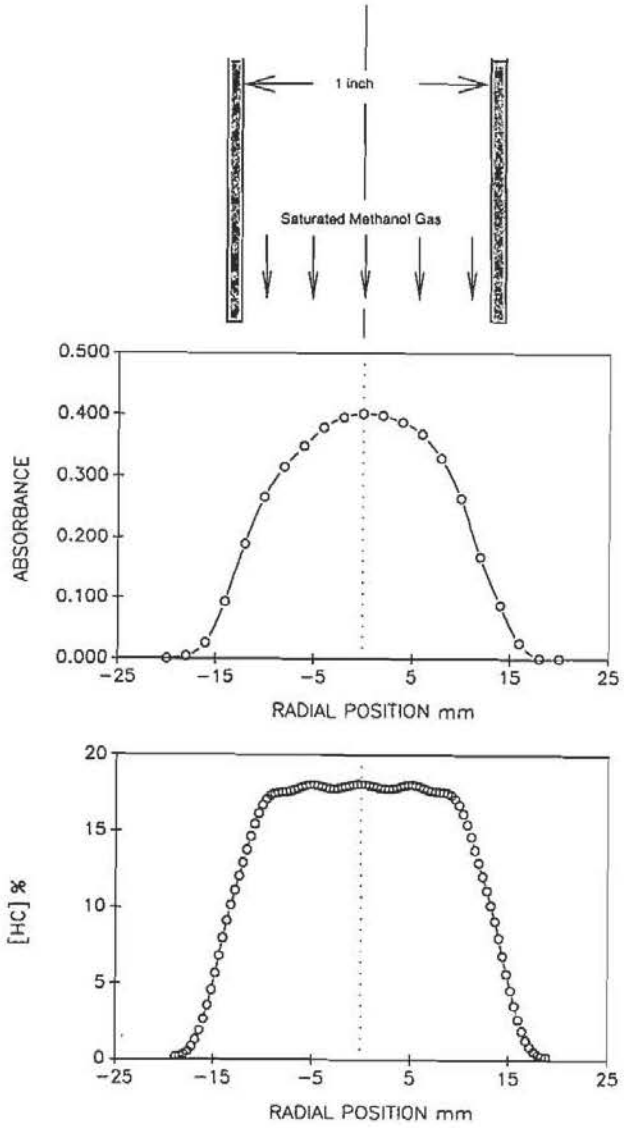

FIGURE 5 Single Phase Jet Results. a) Line-Of-Sight Absorbance b) Deconvoluted Concentration.

the right side of the schematic represents the approximate location of the reaction zone. The spray is produced by a non-swirling air-assist atomizer running 1.26 g/s of methanol with an air to liquid ratio of 1.02. In both cases, the concentration of methanol vapor is measured. The facility utilized in obtaining the measurements is shown in Figure 7 and features a 455 mm square cross section and various window modules which permit a variety of optical measurements, including the one described here, to be conducted.

Non-reacting spray Figure 8a presents a 3D plot of the vapor concentration in the methanol spray. The maximum vapor concentration at each axial location occurs at

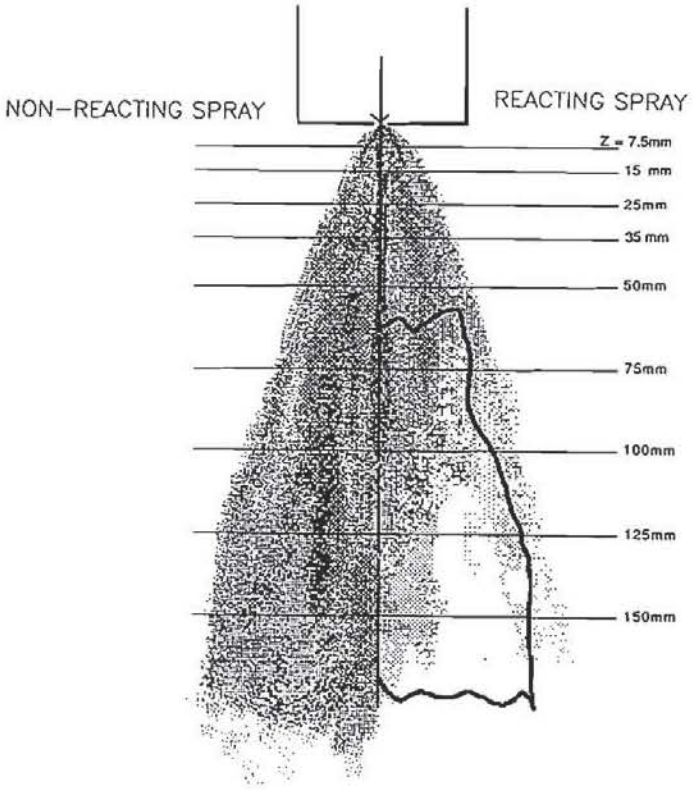

FIGURE 6 Schematic of Spray Structure.

the centerline of the spray. Due to dilution associated with entrained air, the vapor concentration decreases with increased radial distance. The profile spreads radially with increased axial distance due to the mixing at the shear layer between the atomizing air jet and the surrounding air. The flat vapor concentration profile which persists from an axial location of 50 mm and beyond is interpreted as a saturation condition, which would correspond to a gas temperature of -3 to $-5°$C. The saturated assumption is reasonable considering the saturation temperature of methanol at 760 mmHg is $-10°$C.

Reacting spray Figure 8b presents 3D plots of the hydrocarbon concentration in the reacting spray. The results behave in a similar manner to those for the non-reacting case. In the reacting case, however, the peak levels of hydrocarbon vapor increase substantially. Also, instead of a monotonic spread with increased axial distance, the width of the hydrocarbon concentration field first increases and then decreases with axial distance. These differences are due to the presence of reaction which both increases the evaporation of the droplets and also consumes the vapor. The hydrocarbon concentrations measured indicate that the reaction is lean. Overall, the results add great insight into the location of the reaction zone, the manner in which the droplets evaporate, and the way in which the vapor is consumed.

Complementary Results These data are complementary to results obtained with other non-intrusive measurements. As an example, Figure 9 presents radial profiles of

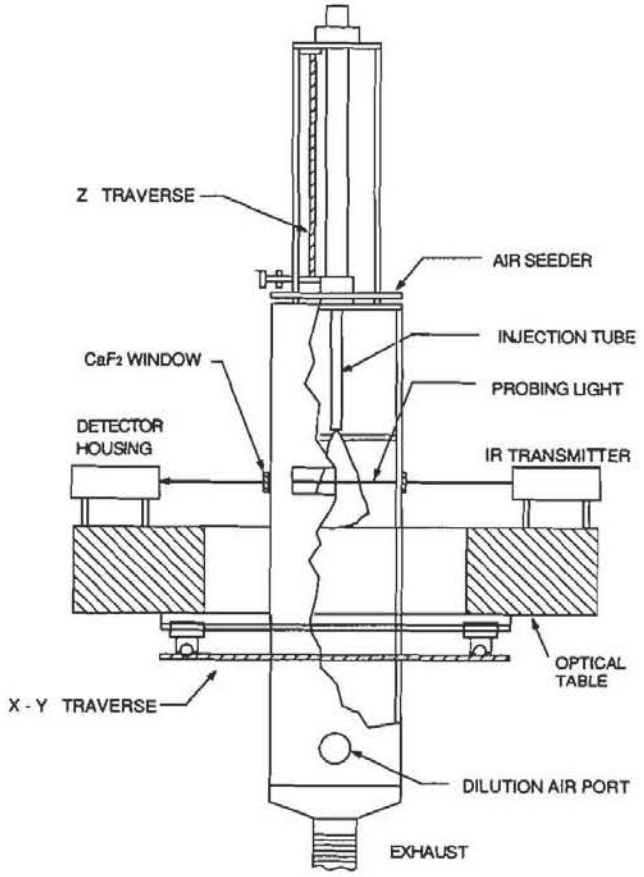

FIGURE 7 Spray Facility.

the hydrocarbon concentration, gas mean axial velocity, and droplet distribution volume mean diameter (D_{30}) for the non-reacting and reacting spray. The results presented in Figure 9b and 9c were obtained using phase Doppler interferometry.

The results reveal similarities in the information obtained from the two diagnostics. For example, the results for the gas axial velocity and the droplet distribution D_{30} indicate that a region near the centerline exists where little difference between the reacting and non-reacting cases is observed. This region extends out radially 6–10 mm, and suggests that no reaction occurs near the centerline at an axial location of 75 mm. The D_{30} values are less affected by the presence of reaction than are the gas velocities and, as a result, the values for the two cases correspond to a radial location of 10 mm. This is due to the relatively small sensitivity of D_{30} to the evaporation of small drops. The gas velocity, on the other hand, increases with the presence of reaction due to the expansion of gases.

The results reveal two distict regions in the reacting spray, (1) a relatively cool central core and (2) an annular reaction zone surrounding the core. In addition to additional insight regarding the physical structure of the spray, the data provide useful and needed information for the development of numerical codes.

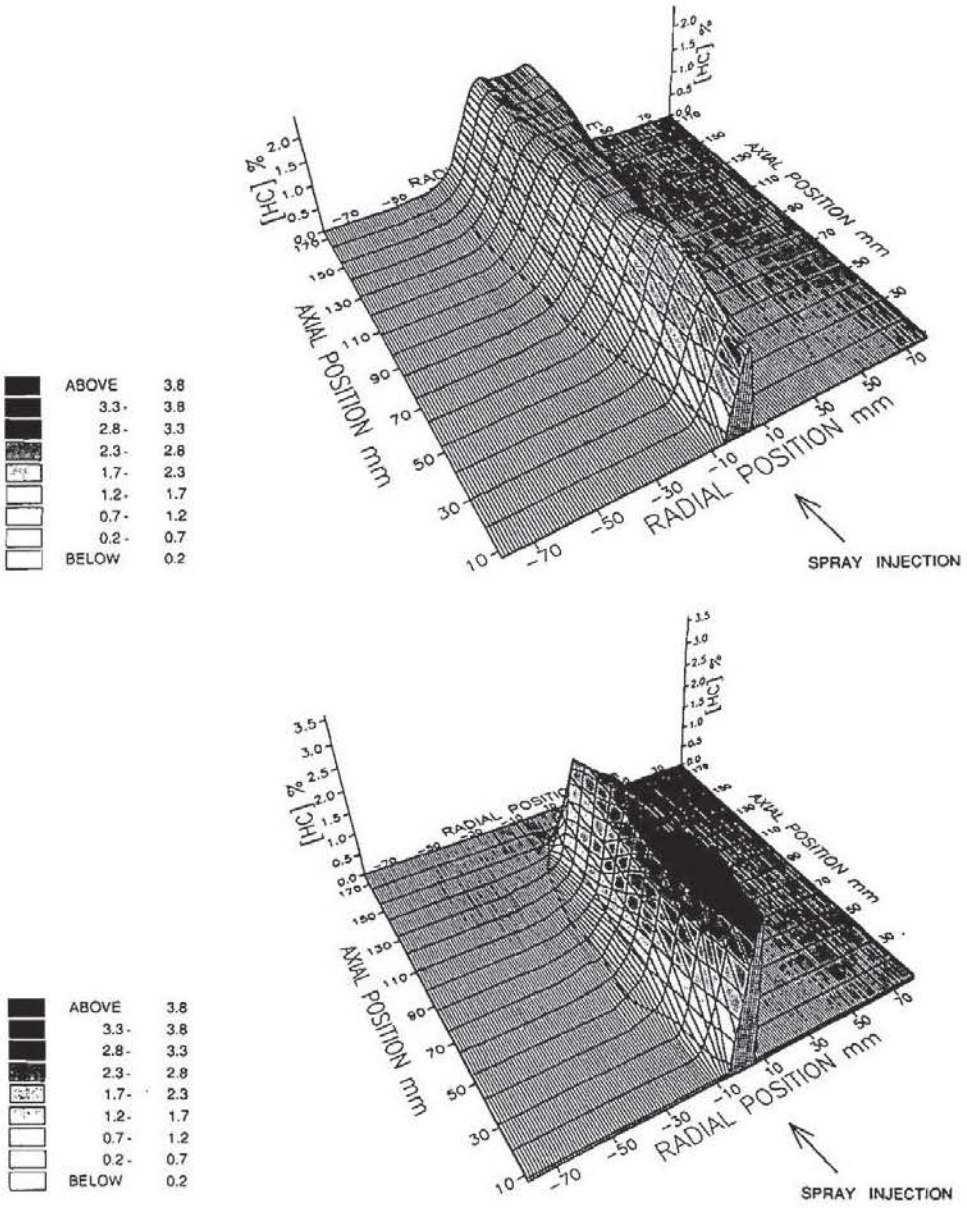

FIGURE 8 Surface Plot of [HC]. a) Non-Reacting Spray b) Reacting Spray.

Combined Results The vapor concentration can also be combined with the gas phase velocity results obtained using phase Doppler interferometry to provide a measure of the vapor mass flux at each point in the spray. Additional details regarding the combination are provided elsewhere (McDonell, 1990). As an example of these results, Figure 10a presents radial profiles of vapor mass flux for the non-reacting methanol spray discussed above. The results show that the vapor flux profiles spread radially with increased axial distance. Because of the continual production of vapor

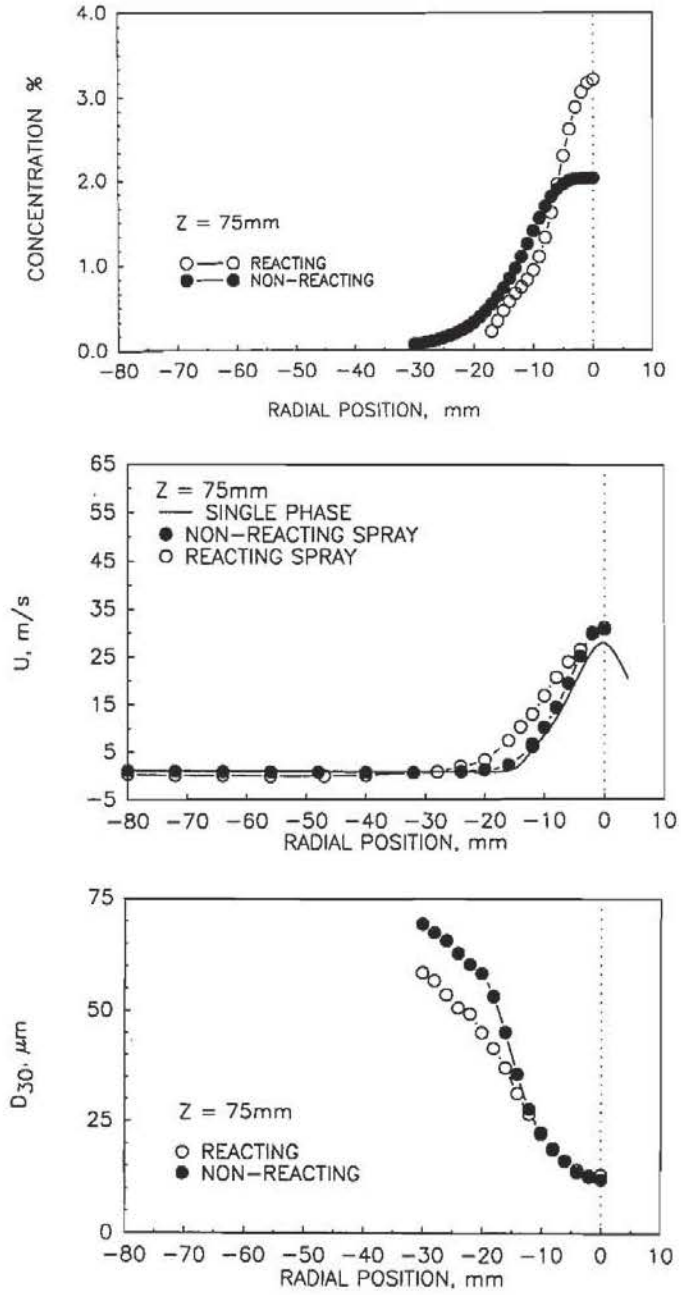

FIGURE 9 Representative Radial Profiles (Axial Distance of 75 mm). a) [HC] b) Gas Mean Velocity c) Droplet Distribution D_{30}

by the drops, the area under each profile must increase. This is illustrated by integrating the profiles in Figure 10a in the radial and azimuthal direction to obtain the mass flow rate of vapor through each axial plane. These results are shown in Figure 10b. The results provide a direct measure of the vaporization of the spray, and, combined

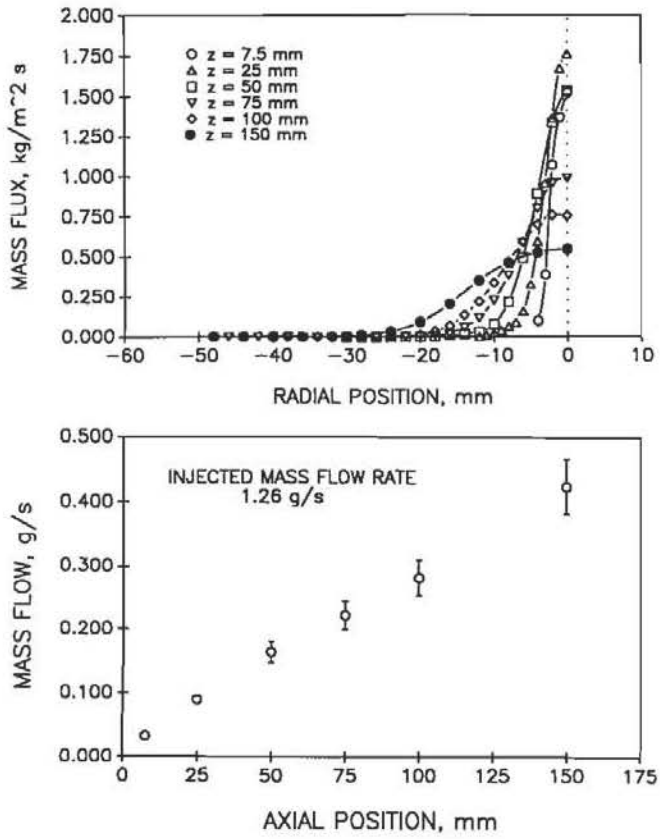

FIGURE 10 Evolution of Vapor (Non-Reacting Case). a) Radial Profiles of Vapor Mass Flux b) Vapor Mass Flow Rate.

with the velocity and size distribution of the drops, can, in principle, be used to verify numerical and empirical vaporization models.

CONCLUSIONS

A non-intrusive techniques, IRES, has been established for providing spatially resolved measurements of gas species concentrations within liquid sprays under reacting and non-reacting conditions. The technique is general enough for application to arbitrary particle laden flows. Three test cases are presented: (1) a single phase jet, (2) a non-reacting methanol spray, and (3) a reacting methanol spray. In each case, the concentration of hydrocarbons present in the flow is measured. IRES can be extended to other species in a straightforward manner. The results demonstrate the capability of the technique and how it can complement and be combined with data obtained with other non-intrusive diagnostic tools.

ACKNOWLEDGEMENTS

The authors acknowledge the support of the Parker Hannifin Corporation for studies associated with spray characterization and two-phase transport and an Air Force Fellowship (F49620-86-C-0127) awarded to

the second author. The contribution of Horiba Limited in supporting the development and application of the technique is greatly appreciated. Discussions with B. Ault, S. Kakigi and Y. Yamagishi regarding the system are also appreciated. M Adachi is a visiting Scientist from Horiba, Ltd., Kyoto Japan.

REFERENCES

Allen, M. G. and Hanson, R. K. (1986). Digital imaging of species concentration fields in spray flames. *Twenty-First Symposium (International) on Combustion*, The Combustion Institute, Pittsburgh, PA, 1755.

Bachalo, W. D., and Houser, M. J. (1984). Phase Doppler spray analyzer for simultaneous measurement of drop size and velocity distributions. *Opt. Engr.* **23**, 583.

Chen, F. P. and Goulard, R. (1976). Retrieval of arbitrary concentration and temperature fields by multiangular scanning techniques. *J. Quant. Spectrosc. Radiat. Transfer*. **16**, 819.

Chraplyvy, A. R. (1981). Non-intrusive measurements of vapor concentrations inside sprays. *Appl. Opt.* **20**, 2620.

McDonell, V. G. (1990). Evolution of droplet/gas phase interaction in polydispersed reacting and non-reacting sprays. Ph.D. dissretation, University of California, Irvine.

McDonell, V. G. and Samuelsen, G. S. (1988). Application of two-component phase Doppler interferometry to the measuremtn of size, velocity, and mass flux in two-phase flows. *Twenty-second Symposium (International) on Comubstion*, The Combustion Institute, Pittsburgh, PA, 1961.

McDonell, V. G. and Samuelsen, G. S. (1989). Influence of the continuous and dispersed phases on the symmetry of a gas turbine air-blast atomizer. *ASME Journal of Engr. Gas Turb. and Power*, **112**, 44.

McDonell, V. G., Adachi, M., and Samuelsen, G. S. (1990). Experimental investigation of a non-swirling, air-assisted methanol spray under reacting and non-reacting conditions. Submitted to *Atomization and Sprays*.

Melton, L. A. and Verdieck, J. F. (1984). Vapor/liquid visualization in fuel sprays. *Twentieth Symposium (International) on Combustion*, The Combustion Institute, Pittsburgh, PA, 1283

Owen, F. K., Spadaccini, L. J., Kennedy, J. B., and Bowman, C. T. (1978). Effects of inlet air swirl and fuel volatility on the structure of confined spray flames. *Seventeenth Symposium (International) on Combustion*, The Combustion Institute, Pittsburgh, PA, 467.

Santoro, R. J., Semerjian, H. G., Emmerman, P. J., and Goulard, R. (1981). Optical tomography of flow field diagnostics. *Int. J. Heat Mass Transfer*, **24**, 1139.

Sethna, P. P. and Williams, D. (1979). Optical constants of alcohols in the infrared. *J. Phys. Chem.* **83**, 405.

Solomon, P. R., *et al.* (1986). FT-IR emission/transmission spectroscopy for in situ combustion diagnostics. *Twenty-First Symposium (International) on Combustion*, The Combustion Institute, Pittsburgh, PA, 1763.

van de Hulst, H. C. (1981). Light scattering by small particles, Dover Publications, Inc., New York.

Wood, C. P., Ault, B. A., and Samuelsen, G. S. (1987). Large angle intensity ratioing for the measurement of particulate size in a combustion environment. in Proceedings of the Sixth International Congress on Applications of Lasers and Electro-Optics. (ICALEO). Vol. 63, Optical Methods in Flow and Particle Diagnostics, pp. 215–224.